



3 **Application of a laser-based spectrometer for continuous insitu**
4 **measurements of stable isotopes of soil CO₂ in calcareous and**
5 **acidic soils**

6 Jobin. Joseph¹, Christoph. Külls², Matthias. Arend³, Marcus. Schaub¹, Frank. Hagedorn¹, Arthur.
7 Gessler¹ and Markus. Weiler⁴

8 [1] {Swiss Federal Institute for Forest, Snow and Landscape Research WSL, Zürcherstrasse 111, 8903
9 Birmensdorf, Switzerland}

10 [2] {Laboratory for Hydrology and International Water Management, University of Applied Sciences Lübeck,
11 Germany}

12 [3] {Physiological Plant Ecology (PPE), Faculty of Integrative Biology, University of Basel, Switzerland}

13 [4] {Chair of Hydrology, Faculty of Environment and Natural resources, University of Freiburg, Germany}

14 Correspondence to: J. Joseph (jobin.joseph@wsl.ch)

15



16 **Abstract**

17 The short-term dynamics of carbon and water fluxes across the soil-plant-atmosphere continuum are still not fully
18 understood. One important constraint is the lack of methodologies that enable simultaneous measurements of soil
19 CO₂ concentration and respective isotopic composition at a high temporal resolution for longer periods of time.
20 δ¹³C of soil CO₂ can be used to derive information on the origin and physiological history of carbon and δ¹⁸O in
21 soil CO₂ aids to infer interaction between CO₂ and soil water. We established a real-time method for measuring
22 soil CO₂ concentration, δ¹³C and δ¹⁸O values across a soil profile at higher temporal resolutions up to 1Hz using
23 an Off-Axis Integrated Cavity Output Spectrometer (OA-ICOS). We also developed a calibration method
24 correcting for the sensitivity of the device against concentration-dependent shifts in δ¹³C and δ¹⁸O values under
25 highly varying CO₂ concentration. The deviations of measured data were modelled, and a mathematical correction
26 model was developed and applied for correcting the shift. By coupling an OA-ICOS with hydrophobic but gas
27 permeable membranes placed at different depths in acidic and calcareous soils, we investigated the contribution of
28 abiotic and biotic components to total soil CO₂ release. We found that in the calcareous Gleysol, CO₂ originating
29 from carbonate dissolution contributed to the total soil CO₂ concentration at detectable degrees probably due to
30 CO₂ evasion from groundwater. Inward diffusion of atmospheric CO₂ was found to be rather pronounced in the
31 topsoil layers at both sites. No specific pattern was identified for δ¹⁸O in soil CO₂ at the calcareous site, δ¹⁸O values
32 reflected fairly well the δ¹⁸O of soil water at the acidic soil site.

33

34 **Key words:** δ¹³C, δ¹⁸O, OA-ICOS, hydrophobic/gas permeable membrane.

35



36 1 Introduction

37 Global fluxes of CO₂ and H₂O are two major driving forces controlling earth's climatic systems. To understand the
38 prevailing climatic conditions and predict climate change, accurate monitoring and modeling of these fluxes are
39 inevitable (Barthel et al., 2014; Harwood et al., 1999; Schär et al., 2004). Approximately 30 - 35% of the global
40 CO₂ flux is contributed by soil CO₂ efflux, which is, therefore, a significant determinant of the net ecosystem
41 carbon balance (Schlesinger and Andrews, 1999). The long-term dynamics of CO₂ release on a seasonal scale are
42 reasonably well understood (Satakhun et al., 2013), whereas less information on CO₂ dynamics and isotopic
43 composition are available for short-term variations on a diurnal scale (Werner and Gessler, 2011). The lack of
44 proper understanding of the diurnal fluctuations in soil CO₂ release might introduce uncertainty in estimating the
45 soil carbon budget and the CO₂ fluxes to the atmosphere. The isotopic composition of soil CO₂ and its diel
46 fluctuation can be a critical parameter for the partitioning of ecosystem gas exchange into its components (Bowling
47 et al., 2003; Mortazavi et al., 2004) and for disentangling plant and ecosystem processes (Werner and Gessler
48 2011). By assessing $\delta^{13}\text{C}$ of soil CO₂, it is possible to identify the source for CO₂ (Kuzyakov, 2006) and the
49 coupling between photosynthesis and soil respiration when taking into account post-photosynthetic isotope
50 fractionation (Werner et al., 2012; Wingate et al., 2010). $\delta^{13}\text{C}$ soil CO₂ reflects, however, not only microbial and
51 root respiration but also abiotic sources from carbonate weathering (Schindlbacher et al., 2015).

52 Soil water imprints its $\delta^{18}\text{O}$ signature on soil CO₂ as a result of isotope exchange between H₂O and CO₂ (aqueous).
53 The oxygen isotopic exchange between CO₂ and soil water is catalyzed by microbial carbonic anhydrase (Sperber
54 et al., 2015; Wingate et al., 2009). Thus, soil CO₂ can give information on the isotopic composition of both soil
55 water resources and Carbon sources. The oxygen isotope composition of plant-derived CO₂ is both, a tracer of
56 photosynthetic and respiratory CO₂ and gives additional quantitative information on the water cycle in terrestrial
57 ecosystems (Francey and Tans, 1987). To better interpret the $\delta^{13}\text{C}$ and $\delta^{18}\text{O}$ signals of atmospheric CO₂, the
58 isotopic composition and its variability of the different sources need to be better understood (Werner et al., 2012;
59 Wingate et al., 2010).

60 The conventional method to estimate $\delta^{13}\text{C}$ and $\delta^{18}\text{O}$ of soil CO₂ efflux is by using two end-member mixing models
61 of atmospheric CO₂ and CO₂ produced in the soil (Keeling, 1958). The conventional methods for sampling soil
62 produced CO₂ are chamber based (Bertolini et al., 2006; Torn et al., 2003) and 'mini-tower' (Kayler et al., 2010;
63 Mortazavi et al., 2004) based methods. In all these conventional methods, air sampling is done at specific time
64 intervals, and $\delta^{13}\text{C}$ and $\delta^{18}\text{O}$ are analyzed using Isotope Ratio Mass Spectrometry (IRMS) (Ohlsson et al., 2005).
65 Such offline methods have several disadvantages like high sampling costs, excessive time consumption for
66 sampling and analysis, increased sampling error and low temporal resolution. Kammer et al. showed how error-
67 prone could the conventional methods be while calculating $\delta^{13}\text{C}$ and $\delta^{18}\text{O}$ (up to several per mil when using
68 chamber and mini tower-based methods) (Kammer et al., 2011). In chamber-based systems, non-steady-state
69 conditions may arise within the chamber due to increased CO₂ concentrations which in turn hinders the diffusion
70 of ¹²CO₂ more strongly than that of heavier ¹³CO₂ (Risk and Kellman, 2008). Moreover, it has been found that



71 $\delta^{18}\text{O}$ of CO_2 inside a chamber is significantly influenced by the $\delta^{18}\text{O}$ of the surface soil water as an equilibrium
72 isotopic exchange happens during the upward diffusive movement of soil CO_2 (Mortazavi et al., 2004).

73 The advent of laser-based isotope spectroscopy has enabled cost-effective, simple, and high precision real-time
74 measurements of $\delta^{13}\text{C}$ and $\delta^{18}\text{O}$ in CO_2 (Kammer et al., 2011; Kerstel and Gianfrani, 2008). This technique opened
75 up new possibilities for faster and reliable measurements of stable isotopes, based on the principle of light
76 absorption, using laser beams of distinct wavelengths in the near and mid-infrared range (Bowling et al., 2003).

77 In 1988, O'Keefe and Decon introduced the Cavity Ring-Down Spectroscopy (CRDS) for measuring the isotopic
78 ratio of different gaseous species based on laser spectrometry (O'Keefe and Deacon, 1988). With the laser-based
79 spectrometry techniques, measuring sensitivities up to parts per trillion (ppt) concentrations are achieved (von
80 Basum et al., 2004; Peltola et al., 2012). In CRDS, the rate of change in the absorbed radiation of laser light that
81 is temporarily "trapped" within a highly reflective optical cavity is determined. This is achieved using resonant
82 coupling of a laser beam to the optical cavity and active locking of laser frequency to cavity length (Parameswaran
83 et al., 2009). Another well-established technique similar to CRDS is Off-Axis Integrated Cavity Output
84 Spectroscopy (OA-ICOS). It is based on directing lasers with narrowband and continuous-wave in an off-axis
85 configuration to the optical cavity (Baer et al., 2002).

86 Even though OA-ICOS can measure concentration and isotope signature of various gaseous species at high
87 temporal resolution, we found pronounced deviations in $\delta^{13}\text{C}$ and $\delta^{18}\text{O}$ measurements from the absolute values
88 when measured under changing CO_2 concentrations. So far to our knowledge, no study has been made available
89 detailing the calibration process of OA-ICOS CO_2 analyzers correcting for fluctuations of $\delta^{13}\text{C}$ and $\delta^{18}\text{O}$ values
90 under varying CO_2 concentrations. Most of the OA-ICOS CO_2 analyzers are built for working under stable CO_2
91 concentrations, so that periodical calibration against in-house gas standards at a particular concentration is
92 sufficient. However, as there are pronounced gradients in CO_2 levels in soils (Maier and Schack-Kirchner, 2014),
93 CO_2 concentration depending shifts in measured isotopic values have to be addressed and corrected. Such
94 calibration is, however, also relevant for any other OA-ICOS application with varying levels of CO_2 (e.g., in
95 chamber measurements). Hence the first part of this work comprises the establishment of a calibration method for
96 OA-ICOS. The second part describes a method for online measurement of CO_2 concentrations and stable carbon
97 and oxygen isotope composition of CO_2 in different soil depths by coupling OA-ICOS with gas permeable
98 hydrophobic tubes (Membrane tubes, Accurel®). The use of these tubes for measuring soil CO_2 concentration (Gut
99 et al., 1998) and $\delta^{13}\text{C}$ of soil CO_2 (Parent et al., 2013) has already been established, but the coupling to an OA-
100 ICOS system has not been performed, yet.

101 We evaluated our measurement system by assessing and comparing the concentration, $\delta^{13}\text{C}$ and $\delta^{18}\text{O}$ of soil CO_2
102 for a calcareous and an acidic soil system. The primary foci of this study are to (1) introduce OA-ICOS in online
103 soil CO_2 concentration and isotopic measurements; (2) calibrate the OA-ICOS to render it usable for isotopic
104 analysis carried out under varying CO_2 concentrations; and (3) analyze the dynamics of $\delta^{13}\text{C}$ and $\delta^{18}\text{O}$ of soil CO_2
105 at different soil depths in different soil types at a higher temporal resolution.

106



107 2 Materials and Methods

108 2.1 Instrumentation

109 The concentration, $\delta^{13}\text{C}$ and $\delta^{18}\text{O}$ values of CO_2 were measured with an OA-ICOS, as described in detail by Baer
110 et al. and Jost et al. (Baer et al., 2002; Jost et al., 2006). In this study, we used an OA-ICOS, (LGR-CCIA 36-d)
111 manufactured by Los Gatos Research Ltd, San-Francisco, USA. LGR-CCIA 36-d measures CO_2 concentration,
112 and $\delta^{13}\text{C}$ and $\delta^{18}\text{O}$ values at a frequency up to 1 Hz. The operational CO_2 concentration range was 400 to 25,000
113 ppm. Operating temperature range was +10 - +35°C, and sample temperature range (Gas temperature) was between
114 -20°C and 50°C. Recommended inlet pressure was < 0.0689 MPa. The multiport inlet unit, an optional design that
115 comes along with LGR-CCIA 36-d, had a manifold of 8 digitally controlled inlet ports and one outlet port. It
116 rendered the user with an option of measuring eight different CO_2 samples at the desired time interval. Three
117 standard gases with distinct $\delta^{13}\text{C}$ and $\delta^{18}\text{O}$ values were used for calibration in this study (See Table.1). The standard
118 gases used in this study were analyzed for absolute concentration and respective $\delta^{13}\text{C}$ and $\delta^{18}\text{O}$ values. δ -values
119 are expressed based on Vienna Pee Dee Belemnite (VPDB)- CO_2 scale, and were determined by high precision
120 IRMS analysis.

121 2.2 Calibration setup and protocol

122 We developed a two-step calibration procedure to; a) correct for concentration-dependent error in isotopic data
123 measurements, and b) correct for deviations in measured δ -values from absolute values due to offset (other than
124 concentration-dependent error) introduced by the laser spectrometer. Also, we used Allan variance curves for
125 determining the time interval to average the data to achieve the highest precision that can be offered by LGR-CCIA
126 36-d (Allan et al., 1997).

127 First part of our calibration methodology was developed to correct for the concentration-dependent error observed
128 in preliminary studies for $\delta^{13}\text{C}$ and $\delta^{18}\text{O}$ values measured using OA-ICOS. Such a calibration protocol was used
129 in addition to the routine three-point calibration performed with in-house CO_2 gas standards of known $\delta^{13}\text{C}$ and
130 $\delta^{18}\text{O}$ values. We developed a CO_2 dilution set up (See Figure. 1), with which each of the three CO_2 standard gases
131 was diluted with N_2 gas to different CO_2 concentrations. By applying a dilution series, we identified the deviation
132 of the measured from the absolute $\delta^{13}\text{C}$ and $\delta^{18}\text{O}$ values depending on CO_2 concentration (See Figure.4). $\delta^{13}\text{C}$, and
133 $\delta^{18}\text{O}$ of the standard gases across a wide range of CO_2 concentrations are measured. The deviation of the measured
134 $\delta^{13}\text{C}$, and $\delta^{18}\text{O}$ from absolute values with respect to changing CO_2 concentrations were mathematically modeled
135 and later used for data correction (See Figure.5). A standard three-point calibration is then applied correcting for
136 concentration-dependent error (See Figure.7). The standards used covered a wide range of $\delta^{13}\text{C}$ and $\delta^{18}\text{O}$,
137 including the values observed in the field of application.

138 Standard gases were released to a mass flow controller (ANALYT-MTC, series 358, MFC1) after passing through
139 a pressure controller valve (See Figure. 1) with safety bypass (TESCOM, D43376-AR-00-X1-S; V5). A 0.5 μm
140 filter with a PTFE membrane, ((Stainless Steel All-Welded In-Line Filter (Swagelok, SS-4FWS-05; F1)) was
141 installed at the inlet of the flow controller (ANALYT-MTC, series 358; MFC1) to prevent moisture from getting



142 into the device. N₂ gas was released and passed to another flow controller (ANALYT-MTC, series 358; MFC2)
143 through a 0.5 µm PTFE membrane filter (F2 in Figure. 1). CO₂ and N₂ gases leaving the flow controllers (MFC1
144 and MFC2 respectively) were then mixed and drawn through a ¼" Teflon tube (P8) which is kept in a thermostat-
145 controlled water bath (Kottermann, 3082) to the multiport inlet unit of OA-ICOS. By using the water bath, we
146 were able to adjust the reference gas temperature between -20 - +40°C and test the temperature sensitivity of the
147 δ¹³C and δ¹⁸O measurements. The third CO₂ standard gas was produced by mixing the other two gas standards in
148 equal molar proportions and was mixed in a 10L volume plastic bag with inner aluminum foil coating and welded
149 seams (CO₂ mix: Linde PLASTIGAS®) under 0.03 MPa pressure by diluting to the required concentration using
150 N₂ gas. The mixture was then temperature adjusted and delivered to the multiport inlet unit by using a ¼" Teflon
151 tube (P10). From the multiport inlet unit, calibration gases were delivered into LGR-CCIA 36-d for measurement
152 using a ¼" Teflon tube (P9) at a pressure < 0.0689 MPa, with a flow rate of 500 mL/min. CO₂ gas standards were
153 measured at varying concentration between 400 and 25,000 ppm. Every hour before sampling, N₂ gas was flushed
154 through the system to remove CO₂ to avoid memory effect. The three calibration gases measured in a sequence
155 one after the other four times. During each round of measurement, every calibration gas was diluted to different
156 concentrations of CO₂ (400 - 25,000 ppm) and measured respective isotopic signature and concentration. For each
157 measurement of δ¹³C and δ¹⁸O at a given concentration, the first 50 readings were omitted to avoid possible
158 memory effects of the laser spectrometer and the subsequent readings for the next 256 seconds were taken and
159 averaged to get maximum precision for δ¹³C and δ¹⁸O measurements. When switching between different
160 calibration gases at the multiport inlet unit, N₂ gas was purged through the systems for 30 seconds to avoid cross-
161 contamination.

162 2.3 Experimental Sites

163 In situ experiments were conducted to measure δ¹³C, δ¹⁸O and concentration of soil CO₂ in two different soil types
164 (calcareous and acidic soil). In situ field measurements in a calcareous soil were conducted during June 2014 in
165 cropland cultivated with wheat (*Triticum aestivum*) in Neuried, a small village in the Upper Rhine Valley in
166 Germany situated at 48°26'55.5"N, 7°47'20.7"E, 150 m a.s.l. The soil type described as calcareous fluvic Gleysol
167 developed on gravel deposits in the upper Rhine valley. Soil depth was medium to deep, with high contents of
168 coarse material (> 2 mm) up to 30 - 50%. Mean soil organic carbon (SOC) content was 1.2 - 2% and, SOC stock
169 was ranging between 50 and 90 t/ha. The average pH was found to be 8.6. The study site receives an annual
170 rainfall of 810 mm and has a mean annual temperature of 12.1°C.

171 In situ measurements in an acidic soil were conducted by the end of July 2014 in the model ecosystem facility
172 (MODOEK) of the Swiss Federal Research Institute WSL, Birmensdorf, Switzerland (47°21'48" N, 8°27'23" E,
173 545 m a.s.l.). The MODOEK facility comprises 16 model ecosystems, belowground split into two lysimeters with
174 an area of 3 m² and a depth of 150 cm. The lysimeters used for the present study were filled with acidic (haplic



175 Alisol) forest soil and planted with young beech trees (Arend et al., 2016). The soil pH was 4.0 and a total SOC
176 content of 0.8% (Kuster et al., 2013).

177 2.4 Experimental Setup

178 OA-ICOS was connected to gas permeable, hydrophobic membrane tubes (Accurel® tubings, 8 mm OD) of 2 m
179 length, placed horizontally in the soil at different depths. Tubes were laid in six different depths (4, 8, 12, 17, 35,
180 and 80 cm) for calcareous soil and three (10, 30, and 60 cm) for acidic soil.

181 Technical details of measurement setup were shown in Figure 2. Both ends of the membrane tubes were extended
182 vertically upwards reaching the soil top by connecting them to gas impermeable Synflex® tubings (8 mm OD)
183 using Swagelok tube fitting union (Swagelok: SS-8M0-6, 8 mm Tube OD). One end of the tubing system was
184 connected to a solenoid switching valve (Bibus: MX-758.8E3C3KK) by using a stainless steel reducing union
185 (Swagelok: SS-8M0-6-6M), to the outlet of the LGR CCIA 36-d by using ¼" Teflon tubing. The other end was
186 connected via the multiport inlet unit to the gas inlet of the LGR CCIA 36-d.

187 This way, a loop was created in which the soil CO₂ drawn into the OA-ICOS was circulated back through the tubes
188 and in and out of the OA-ICOS and measured until a steady state was reached. Each depth was selected and
189 continuously measured for 6 minutes at specified time intervals by switching to defined depths at the multiport
190 inlet unit and also at the solenoid valve.

191

192 3 Results and Discussion

193 The highest level of precision obtained for $\delta^{13}\text{C}$ and $\delta^{18}\text{O}$ measurements at the maximum measuring frequency
194 (1Hz) were determined by using Allan deviation curves (see Figure 3). Maximum precision of 0.022‰ for $\delta^{13}\text{C}$
195 was obtained when the data were averaged over 256 seconds, and for $\delta^{18}\text{O}$, 0.077‰ for the same averaging interval
196 as for $\delta^{13}\text{C}$.

197 To correct for CO₂ concentration-dependent error in raw $\delta^{13}\text{C}$ and $\delta^{18}\text{O}$ data, we analysed data obtained from the
198 OA-ICOS to determine the sensitivity of $\delta^{13}\text{C}$ and $\delta^{18}\text{O}$ measurements against changing concentrations of CO₂. We
199 observed a specific pattern of deviance in the measured isotopic data from the absolute values (both for $\delta^{13}\text{C}$ and
200 $\delta^{18}\text{O}$) across CO₂ concentration ranging from 25,000 to 400 ppm (See Figure.4). Uncalibrated $\delta^{13}\text{C}$ and $\delta^{18}\text{O}$
201 measurements showed a standard deviation of 8.1‰ and 4.7‰ respectively, when measured under changing CO₂
202 concentrations.

203 The dependency of $\delta^{13}\text{C}$ and $\delta^{18}\text{O}$ values on the CO₂ concentration was compensated by using a nonlinear model.
204 The deviations ($\Delta\delta$) of the measured delta values (δ_{M}) from the absolute value of the standard gas (δ_{R}) at different
205 concentrations of CO₂ were calculated ($\Delta\delta = \delta_{\text{M}} - \delta_{\text{R}}$). Several mathematical models were then fitted on $\Delta\delta$ as a
206 function of changing CO₂ concentration (See figure.5). The mathematical model most fitting to the ($\Delta\delta$) data was
207 selected using Akaike information criterion corrected (AICc) (Glatting et al., 2007; Hurvich and Tsai, 1989;
208 Yamaoka et al., 1978). The non-linear model fits applied for $\Delta\delta^{13}\text{C}$, and $\Delta\delta^{18}\text{O}$ measurements are given in Tables
209 2 & 3, respectively. For $\Delta\delta^{13}\text{C}$, a three-parameter exponential model fitted best with $r^2 = 0.98$ (see Table 4 for the



210 values of the parameters), and a two-parameter logarithmic model (see Table 3) with $r^2 = 0.99$ showed the best fit
211 for $\Delta\delta^{18}\text{O}$ (see Table 4 for the values of the parameters). The most fitting model was then introduced into the
212 measured isotopic data ($\delta^{13}\text{C}$ and $\delta^{18}\text{O}$) and were corrected for concentration-dependent error (See figure. 6). After
213 correction, the standard deviation of $\delta^{13}\text{C}$ was reduced to 0.98‰ and of $\delta^{18}\text{O}$ to 0.73‰ for all measurements across
214 the whole CO_2 concentration range.

215

216 After correcting the measured $\delta^{13}\text{C}$ and $\delta^{18}\text{O}$ values for the CO_2 concentration-dependent deviations, a three-point
217 calibration was made by generating linear regressions with the concentration corrected $\delta^{13}\text{C}$ and $\delta^{18}\text{O}$ values against
218 absolute $\delta^{13}\text{C}$ and $\delta^{18}\text{O}$ values (See Figure.7). Three-point calibration improved the accuracy further by reducing
219 the standard deviation to 0.935 ‰ for $\delta^{13}\text{C}$ and 0.719 ‰ for $\delta^{18}\text{O}$.

220 During our experiments with the LGR CCIA 36-d, we found that routine calibration (Correction for concentration-
221 dependent error plus three-point calibration) was inevitable for obtaining better accuracy, in particular under
222 fluctuating CO_2 concentrations. The LGR CCIA-36d offers an option for calibration against a single standard, a
223 feature which was already in place in a predecessor model (CCIA DLT-100) (Guillon et al., 2012). This internal
224 calibration is sufficient, when LGR CCIA-36d is operated only under stable CO_2 concentrations. To correct for the
225 concentration dependency, we had introduced mathematical model fits, which corrected for the deviation pattern
226 found for both $\delta^{13}\text{C}$ and $\delta^{18}\text{O}$. We assume that these correction models were instrument specific and a similar
227 procedure needs to be developed for every single device. Experiments conducted to investigate the influence of
228 temperature on $\delta^{13}\text{C}$ and $\delta^{18}\text{O}$ measurements did not show any statistically significant influence. The previous
229 version of the Los Gatos CCIA was strongly influenced by temperature fluctuations during sampling (Guillon et
230 al., 2012). The lack of temperature dependency as observed here with the most recent model is mostly due to the
231 heavy insulation provided with the system, which was not found in the older models.

232 Guillon et al. (2012) found a linear correlation between CO_2 concentration and respective stable isotope signatures
233 with a previous version of Los Gatos CCIA CO_2 stable isotope analyser. In our experiments with LGR CCIA 36-
234 d, best fitting correlation between CO_2 concentration and $\delta^{13}\text{C}$ and $\delta^{18}\text{O}$ measurements were exponential and
235 logarithmic relations, respectively. We assume that measurement accuracy is influenced by the number of CO_2
236 molecules present inside the laser cavity of the particular laser spectrometer as we observed large standard
237 deviation in isotopic measurements at lower CO_2 concentrations. This behavior of an OA-ICOS can be expected
238 as it functions by sweeping the laser along an absorption spectrum, measuring the energy transmitted after passing
239 through the sample. Therefore, energy transmitted is proportional to the gas concentration in the cavity. The laser
240 absorbance is then determined by normalizing against a reference signal, finally calculating the concentration of
241 the sample measured by integrating the whole spectrum of absorbance (O'Keefe et al., 1999).

242 Figures 8 and 9 show the CO_2 concentration, $\delta^{13}\text{C}$ and $\delta^{18}\text{O}$ measurements of soil CO_2 in the calcareous as well as
243 in the acidic soil across the soil profile with sub-daily resolution and as averages for the day, respectively. We
244 observed a linear increase in the CO_2 concentration across the soil depth profile for both, the calcareous and the
245 acidic soil. Moreover, there were rather contrasting $\delta^{13}\text{C}$ values across the profile for the two soil types. In the
246 calcareous soil, CO_2 was relatively enriched in ^{13}C in the surface soil (4 cm) as compared to the 8 cm depth. Below
247 12 cm down to 80 cm depth, we found an increase in $\delta^{13}\text{C}$ values. At 80 cm depth, the $\delta^{13}\text{C}$ in soil CO_2 ranged



248 between -5 and 0‰ (See Figure. 8) with a daily average of -2.63 ± 0.14 ‰ (See Figure. 9) and hence clearly above
249 atmospheric values (≈ -8.0 ‰). No specific pattern was identified for $\delta^{18}\text{O}$ values for the calcareous soil across the
250 profile. While there was a tendency for $\delta^{18}\text{O}$ to decrease with soil depths down to 35 cm, the highest $\delta^{18}\text{O}$ values
251 were observed at 80 cm depth. The patterns observed for the $\delta^{13}\text{C}$ values of CO_2 in the calcareous soil with ^{13}C
252 enrichment in deeper soil layers can be explained by a substantial contribution of CO_2 from abiotic origin to total
253 soil CO_2 release as a result of carbonate weathering and subsequent out-gassing from soil water (Schindlbacher et
254 al., 2015). Carbonates have a distinct $\delta^{13}\text{C}$ value close to 0‰ vs. VPDB, while CO_2 released during respiratory
255 processes has usually $\delta^{13}\text{C}$ values around -24‰ as observed in the acidic soil (Figure 8). Even though the
256 contribution of CO_2 from abiotic sources to soil CO_2 is considered to be low, several studies have reported
257 significant proportions ranging between (10 - 60%) emanating from abiotic sources (Emmerich, 2003; Plestenjak
258 et al., 2012; Ramnarine et al., 2012; Serrano-Ortiz et al., 2010; Stevenson and Verburg, 2006; Tamir et al., 2011).
259 Water content and soil CO_2 concentration are two major factors influencing carbonate weathering, and variations
260 in soil CO_2 partial pressure, moisture, temperature, and pH can cause degassing of CO_2 which contributes to the
261 soil CO_2 efflux (Schindlbacher et al., 2015). We assume that at our study site, the topsoil is de-carbonated due to
262 intensive agriculture for a longer period and thus soil CO_2 there originates primarily from autotrophic and
263 heterotrophic respiratory activity. In contrast to the deeper soil layers, where the carbonate content is high, CO_2
264 from carbonate weathering is assumed to dominate soil CO_2 . Also, outgassing of CO_2 from the large groundwater
265 body underneath the calcareous Gleysol might contribute to the inorganic CO_2 sources in the deeper soil as we
266 found ground water table to be 1-2m below the soil surface. Relative ^{13}C enrichment of the CO_2 in the topsoil (4
267 cm) compared to 8 cm depth is probably due to the invasive diffusion of atmospheric CO_2 which has a $\delta^{13}\text{C}$ value
268 close to -8‰ (e.g., (Levin et al., 1995)). The $\delta^{18}\text{O}$ patterns for CO_2 between 4 and 35 cm might reflect the $\delta^{18}\text{O}$ of
269 soil water with stronger evaporative enrichment at the top and ^{18}O depletion towards deeper soil layers. In
270 comparison, the strong ^{18}O enrichment of soil CO_2 towards 80 cm in the calcareous Gleysol very likely reflects
271 the ^{18}O values of groundwater lending further support for the high contribution of CO_2 originating from the
272 outgassing of groundwater.

273

274 Soil CO_2 concentration in the acidic soil showed a positive relationship with soil depth as CO_2 concentration
275 increased along with increasing soil depth (Figs. 8 & 9). CO_2 concentrations were distinctly higher than in the
276 calcareous soil, very likely due to the finer texture than in the gravel-rich calcareous soil. $\delta^{13}\text{C}$ values increased
277 slightly with soil depths and amounted to approx. - 24‰ in 30 and 80 cm depth indicating the biotic origin from
278 (autotrophic and heterotrophic) soil respiration (Schönwitz et al., 1986). In the topsoil, $\delta^{13}\text{C}$ values did not strongly
279 increase, pointing towards a less pronounced inward diffusion of CO_2 in the acidic soil site, most likely due to
280 more extensive outward diffusion of soil CO_2 as indicated by the still very high CO_2 concentration at 10 cm creating
281 a sharp gradient between soil and atmosphere. Moreover, the acidic soil was rather dense and contained no stones,
282 strongly suggesting that gas diffusivity was rather small. $\delta^{18}\text{O}$ depths patterns of soil CO_2 in the acidic soil were
283 most likely reflecting $\delta^{18}\text{O}$ values of soil water as CO_2 became increasingly ^{18}O depleted from top to bottom. $\delta^{18}\text{O}$
284 of deeper soil layers CO_2 (30 - 60 cm) was close to the values expected when full oxygen exchange between soil
285 water and CO_2 occurred. Irrigation water $\delta^{18}\text{O}$ amounted to $\approx -10 \pm 2$ ‰ against the VSMOW scale and assuming
286 an ^{18}O fractionation of 41‰ between CO_2 and water (Brenninkmeijer et al., 1983) this would result in expected



287 value for CO₂ of $\approx -10 \pm 2\%$ vs. VPDB-CO₂. Corresponding results had been shown for $\delta^{18}\text{O}$ of soil CO₂ using
288 similar hydrophobic gas permeable membrane tubes used when measuring $\delta^{18}\text{O}$ of soil CO₂ and soil water *in situ*
289 (Gangi et al., 2015).

290 4 Conclusions

291 During our preliminary tests with OA-ICOS, we found that the equipment is highly sensitive to changes in CO₂
292 concentrations. Therefore, we developed a calibration strategy for correcting errors introduced in $\delta^{13}\text{C}$ and $\delta^{18}\text{O}$
293 measurements due to the sensitivity of the device against changing CO₂ concentrations. Also, we developed a
294 three-point calibration method for correcting aberrations in $\delta^{13}\text{C}$ and $\delta^{18}\text{O}$ measurements observed in addition to
295 concentration sensitivity. Thus, we introduced a calibration method for OA-ICOS (LGR CCIA 36-d) to measure
296 $\delta^{13}\text{C}$ and $\delta^{18}\text{O}$ under varying concentrations of CO₂. We found that OA-ICOS measure stable isotopes of CO₂ gas
297 samples with a precision comparable to conventional IRMS. The method described in this work for measuring
298 CO₂ concentration, $\delta^{13}\text{C}$ and $\delta^{18}\text{O}$ values in soil air profiles using OA-ICOS and hydrophobic gas permeable tubes
299 are promising and can be applied for soil CO₂ flux studies. As this set up is capable of measuring continuously for
300 longer time periods at higher temporal resolution (1 Hz), it offers greater potential to investigate the isotopic
301 identity of CO₂ and the interrelation between soil CO₂ and soil water. By using our measurement setup, we could
302 identify abiotic as well as biotic contributions to the soil CO₂ at the calcareous soil. We infer that that degassing
303 of CO₂ from carbonates due to weathering and evasion of CO₂ from groundwater may leave the soil CO₂ with a
304 specific and distinct $\delta^{13}\text{C}$ signature especially when the biotic activity is rather low. This was the case in the
305 calcareous Gleysol studied here as indicated by the much lower CO₂ concentrations as compared to the acidic soil.

306

307

308 Acknowledgements

309 We thank Federal Ministry of Education and Research, Germany (BMBF) and KIT (Karlsruhe Institute of
310 Technology) for providing financial support for the project ENABLE-WCM (Grant Number: 02WQ1205). AG
311 and JJ acknowledge financial support by the Swiss National Science Foundation (SNF; 31003A_159866). We
312 thank Barbara Herbstritt, Hannes Leistert, Emil Blattmann and Jens Lange for outstanding support in getting this
313 project into a reality.

314

315

316

317

318

319

320

321 **References**

322 Allan, D. W., Ashby, N. and Hodge, C. C.: The Science of Timekeeping, Hewlett-Packard, 88
323 [online] Available from:
324 [http://www.allanstime.com/Publications/DWA/Science_Timekeeping/TheScienceOfTimekee](http://www.allanstime.com/Publications/DWA/Science_Timekeeping/TheScienceOfTimekeeping.pdf)
325 [ping.pdf](http://www.allanstime.com/Publications/DWA/Science_Timekeeping/TheScienceOfTimekeeping.pdf), 1997.

326 Arend, M., Gessler, A. and Schaub, M.: The influence of the soil on spring and autumn
327 phenology in European beech, edited by C. Li, *Tree Physiol.*, 36(1), 78–85,
328 doi:10.1093/treephys/tpv087, 2016.

329 Baer, D. S., Paul, J. B., Gupta, M. and O’Keefe, A.: Sensitive absorption measurements in the
330 near-infrared region using off-axis integrated-cavity-output spectroscopy, *Appl. Phys. B Lasers*
331 *Opt.*, 75(2–3), 261–265, doi:10.1007/s00340-002-0971-z, 2002.

332 Barthel, M., Sturm, P., Hammerle, A., Buchmann, N., Gentsch, L., Siegwolf, R. and Knohl, A.:
333 Soil H 2 18 O labelling reveals the effect of drought on C 18 OO fluxes to the atmosphere, *J.*
334 *Exp. Bot.*, 65(20), 5783–5793, doi:10.1093/jxb/eru312, 2014.

335 von Basum, G., Halmer, D., Hering, P., Mürtz, M., Schiller, S., Müller, F., Popp, A. and
336 Kühnemann, F.: Parts per trillion sensitivity for ethane in air with an optical parametric
337 oscillator cavity leak-out spectrometer, *Opt. Lett.*, 29(8), 797, doi:10.1364/OL.29.000797,
338 2004.

339 Bertolini, T., Inglema, I., Rubino, M., Marzaioli, F., Lubritto, C., Subke, J.-A., Peressotti, A.
340 and Cotrufo, M. F.: Sampling soil-derived CO₂ for analysis of isotopic composition: a
341 comparison of different techniques, *Isotopes Environ. Health Stud.*, 42(1), 57–65,
342 doi:10.1080/10256010500503312, 2006.

343 Bowling, D. R., Sargent, S. D., Tanner, B. D. and Ehleringer, J. R.: Tunable diode laser
344 absorption spectroscopy for stable isotope studies of ecosystem–atmosphere CO₂ exchange,
345 *Agric. For. Meteorol.*, 118(1–2), 1–19, doi:10.1016/S0168-1923(03)00074-1, 2003.

346 Brenninkmeijer, C. A. M., Kraft, P. and Mook, W. G.: Oxygen isotope fractionation between
347 CO₂ and H₂O, *Chem. Geol.*, 41, 181–190, doi:10.1016/S0009-2541(83)80015-1, 1983.

348 Emmerich, W. E.: Carbon dioxide fluxes in a semiarid environment with high carbonate soils,
349 *Agric. For. Meteorol.*, 116, 91–102 [online] Available from:
350 <http://citeseerx.ist.psu.edu/viewdoc/download?doi=10.1.1.457.6452&rep=rep1&type=pdf>,
351 2003.



- 352 Francey, R. J. and Tans, P. P.: Latitudinal variation in oxygen-18 of atmospheric CO₂, *Nature*,
353 327(6122), 495–497, doi:10.1038/327495a0, 1987.
- 354 Gangi, L., Rothfuss, Y., Ogée, J., Wingate, L., Vereecken, H. and Brüggemann, N.: A New
355 Method for In Situ Measurements of Oxygen Isotopologues of Soil Water and Carbon Dioxide
356 with High Time Resolution, *Vadose Zo. J.*, 14(8), 0, doi:10.2136/vzj2014.11.0169, 2015.
- 357 Glatting, G., Kletting, P., Reske, S. N., Hohl, K. and Ring, C.: Choosing the optimal fit function:
358 Comparison of the Akaike information criterion and the F-test, *Med. Phys.*, 34(11), 4285–4292,
359 doi:10.1118/1.2794176, 2007.
- 360 Guillon, S., Pili, E. and Agrinier, P.: Using a laser-based CO₂ carbon isotope analyser to
361 investigate gas transfer in geological media, *Appl. Phys. B*, 107(2), 449–457,
362 doi:10.1007/s00340-012-4942-8, 2012.
- 363 Gut, A., Blatter, A., Fahrni, M., Lehmann, B. E., Neftel, A. and Staffelbach, T.: A new
364 membrane tube technique (METT) for continuous gas measurements in soils, *Plant Soil*, 198(1),
365 79–88, doi:10.1023/A:1004277519234, 1998.
- 366 Harwood, K. G., Gillon, J. S., Roberts, A. and Griffiths, H.: Determinants of isotopic coupling
367 of CO₂ and water vapour within a *Quercus petraea* forest canopy, *Oecologia*, 119(1), 109–119,
368 doi:10.1007/s004420050766, 1999.
- 369 Hurvich, C. M. and Tsai, C.: Regression and time series model selection in small samples,
370 *Biometrika*, 76(2), 297–307, doi:10.1093/biomet/76.2.297, 1989.
- 371 Jost, H.-J., Castrillo, A. and Wilson, H. W.: Simultaneous ¹³C/ ¹²C and ¹⁸O/ ¹⁶O isotope ratio
372 measurements on CO₂ based on off-axis integrated cavity output spectroscopy, *Isotopes*
373 *Environ. Health Stud.*, 42(1), 37–45, doi:10.1080/10256010500503163, 2006.
- 374 Kammer, A., Tuzson, B., Emmenegger, L., Knohl, A., Mohn, J. and Hagedorn, F.: Application
375 of a quantum cascade laser-based spectrometer in a closed chamber system for real-time δ¹³C
376 and δ¹⁸O measurements of soil-respired CO₂, *Agric. For. Meteorol.*, 151(1), 39–48,
377 doi:10.1016/j.agrformet.2010.09.001, 2011.
- 378 Kayler, Z. E., Sulzman, E. W., Rugh, W. D., Mix, A. C. and Bond, B. J.: Soil biology and
379 biochemistry., Pergamon. [online] Available from:
380 <https://www.cabdirect.org/cabdirect/abstract/20103097455>, 2010.
- 381 Keeling, C. D.: The concentration and isotopic abundances of atmospheric carbon dioxide in



- 382 rural areas, *Geochim. Cosmochim. Acta*, 13(4), 322–334, doi:10.1016/0016-7037(58)90033-4,
383 1958.
- 384 Kerstel, E. and Gianfrani, L.: Advances in laser-based isotope ratio measurements: selected
385 applications, *Appl. Phys. B*, 92(3), 439–449, doi:10.1007/s00340-008-3128-x, 2008.
- 386 Kuster, T. M., Arend, M., Bleuler, P., Günthardt-Goerg, M. S. and Schulin, R.: Water regime
387 and growth of young oak stands subjected to air-warming and drought on two different forest
388 soils in a model ecosystem experiment, *Plant Biol.*, 15, 138–147, doi:10.1111/j.1438-
389 8677.2011.00552.x, 2013.
- 390 Kuzyakov, Y.: Sources of CO₂ efflux from soil and review of partitioning methods, *Soil Biol.*
391 *Biochem.*, 38(3), 425–448, doi:10.1016/j.soilbio.2005.08.020, 2006.
- 392 Levin, I., Graul, R. and Trivett, N. B. A.: Long-term observations of atmospheric CO₂ and
393 carbon isotopes at continental sites in Germany, *Tellus B*, 47(1–2), 23–34, doi:10.1034/j.1600-
394 0889.47.issue1.4.x, 1995.
- 395 Maier, M. and Schack-Kirchner, H.: Using the gradient method to determine soil gas flux: A
396 review, *Agric. For. Meteorol.*, 192–193, 78–95, doi:10.1016/j.agrformet.2014.03.006, 2014.
- 397 Mortazavi, B., Prater, J. L. and Chanton, J. P.: A field-based method for simultaneous
398 measurements of the $\delta^{18}\text{O}$ and $\delta^{13}\text{C}$ of soil CO₂ efflux, *Biogeosciences*, 1(1), 1–9,
399 doi:10.5194/bg-1-1-2004, 2004.
- 400 O’Keefe, A. and Deacon, D. A. G.: Cavity ring- down optical spectrometer for absorption
401 measurements using pulsed laser sources, *Rev. Sci. Instrum.*, 59(12), 2544–2551,
402 doi:10.1063/1.1139895, 1988.
- 403 Ohlsson, K., Singh, B., Holm, S., Nordgren, A., Lovdahl, L. and Hogberg, P.: Uncertainties in
404 static closed chamber measurements of the carbon isotopic ratio of soil-respired CO, *Soil Biol.*
405 *Biochem.*, 37(12), 2273–2276, doi:10.1016/j.soilbio.2005.03.023, 2005.
- 406 Parameswaran, K. R., Rosen, D. I., Allen, M. G., Ganz, A. M. and Risby, T. H.: Off-axis
407 integrated cavity output spectroscopy with a mid-infrared interband cascade laser for real-time
408 breath ethane measurements, *Appl. Opt.*, 48(4), B73, doi:10.1364/AO.48.000B73, 2009.
- 409 Parent, F., Plain, C., Epron, D., Maier, M. and Longdoz, B.: A new method for continuously
410 measuring the $\delta^{13}\text{C}$ of soil CO₂ concentrations at different depths by laser spectrometry, *Eur.*
411 *J. Soil Sci.*, 64(4), 516–525, doi:10.1111/ejss.12047, 2013.



- 412 Peltola, J., Vainio, M., Ulvila, V., Siltanen, M., Metsälä, M. and Halonen, L.: Off-axis re-entrant
413 cavity ring-down spectroscopy with a mid-infrared continuous-wave optical parametric
414 oscillator, *Appl. Phys. B*, 107(3), 839–847, doi:10.1007/s00340-012-5074-x, 2012.
- 415 Plestenjak, G., Eler, K., Vodnik, D., Ferlan, M., Čater, M., Kanduč, T., Simončič, P. and Ogrinc,
416 N.: Sources of soil CO₂ in calcareous grassland with woody plant encroachment, *J. Soils
417 Sediments*, 12(9), 1327–1338, doi:10.1007/s11368-012-0564-3, 2012.
- 418 Ramnarine, R., Wagner-Riddle, C., Dunfield, K. E. and Voroney, R. P.: Contributions of
419 carbonates to soil CO₂ emissions, *Can. J. Soil Sci.*, 92(4), 599–607, doi:10.4141/cjss2011-025,
420 2012.
- 421 Risk, D. and Kellman, L.: Isotopic fractionation in non-equilibrium diffusive environments,
422 *Geophys. Res. Lett.*, 35(2), L02403, doi:10.1029/2007GL032374, 2008.
- 423 Satakhun, D., Gay, F., Chairungsee, N., Kasemsap, P., Chantuma, P., Thanisawanyangkura, S.,
424 Thaler, P. and Epron, D.: Soil CO₂ efflux and soil carbon balance of a tropical rubber plantation,
425 *Ecol. Res.*, 28(6), 969–979, doi:10.1007/s11284-013-1079-0, 2013.
- 426 Schär, C., Vidale, P. L., Lüthi, D., Frei, C., Häberli, C., Liniger, M. A. and Appenzeller, C.:
427 The role of increasing temperature variability in European summer heatwaves, *Nature*,
428 427(6972), 332–336, doi:10.1038/nature02300, 2004.
- 429 Schindlbacher, A., Borcken, W., Djukic, I., Brandstätter, C., Spötl, C. and Wanek, W.:
430 Contribution of carbonate weathering to the CO₂ efflux from temperate forest soils,
431 *Biogeochemistry*, 124(1–3), 273–290, doi:10.1007/s10533-015-0097-0, 2015.
- 432 Schlesinger, W. and Andrews, J.: Soil Respiration and the Global Carbon Cycle,
433 *Biogeochemistry*, 48, 7–20, doi:10.1023/A:1006247623877, 1999.
- 434 Schönwitzer, R., Stichler, W. and Ziegler, H.: δ¹³C values of CO₂ from soil respiration on sites
435 with crops of C₃ and C₄ type of photosynthesis, *Oecologia*, 69(2), 305–308,
436 doi:10.1007/BF00377638, 1986.
- 437 Serrano-Ortiz, P., Roland, M., Sanchez-Moral, S., Janssens, I. A., Domingo, F., Goddérís, Y.
438 and Kowalski, A. S.: Hidden, abiotic CO₂ flows and gaseous reservoirs in the terrestrial carbon
439 cycle: Review and perspectives, *Agric. For. Meteorol.*, 150(3), 321–329,
440 doi:10.1016/j.agrformet.2010.01.002, 2010.
- 441 Sperber, C. Von, Weiler, M. and Büggemann, N.: The effect of soil moisture, soil particle size,



- 442 litter layer and carbonic anhydrase on the oxygen isotopic composition of soil-released CO₂,
443 *Eur. J. Soil Sci.*, doi:10.1111/ejss.12241, 2015.
- 444 Stevenson, B. A. and Verburg, P. S. J.: Effluxed CO₂-¹³C from sterilized and unsterilized
445 treatments of a calcareous soil, *Soil Biol. Biochem.*, 38(7), 1727–1733,
446 doi:10.1016/j.soilbio.2005.11.028, 2006.
- 447 Tamir, G., Shenker, M., Heller, H., Bloom, P. R., Fine, P. and Bar-Tal, A.: Can Soil Carbonate
448 Dissolution Lead to Overestimation of Soil Respiration?, *Soil Sci. Soc. Am. J.*, 75(4), 1414,
449 doi:10.2136/sssaj2010.0396, 2011.
- 450 Torn, M. S., Davis, S., Bird, J. A., Shaw, M. R. and Conrad, M. E.: Automated analysis
451 of ¹³C/¹²C ratios in CO₂ and dissolved inorganic carbon for ecological and environmental
452 applications, *Rapid Commun. Mass Spectrom.*, 17(23), 2675–2682, doi:10.1002/rcm.1246,
453 2003.
- 454 Werner, C. and Gessler, A.: Diel variations in the carbon isotope composition of respired CO₂
455 and associated carbon sources: a review of dynamics and mechanisms, *Biogeosciences*, 8(9),
456 2437–2459, doi:10.5194/bg-8-2437-2011, 2011.
- 457 Werner, C., Schnyder, H., Cuntz, M., Keitel, C., Zeeman, M. J., Dawson, T. E., Badeck, F. W.,
458 Brugnoli, E., Ghashghaie, J., Grams, T. E. E., Kayler, Z. E., Lakatos, M., Lee, X., Maguas, C.,
459 Ogee, J., Rascher, K. G., Siegwolf, R. T. W., Unger, S., Welker, J., Wingate, L. and Gessler,
460 A.: Progress and challenges in using stable isotopes to trace plant carbon and water relations
461 across scales, *Biogeosciences*, 9(8), 3083–3111, doi:10.5194/bg-9-3083-2012, 2012.
- 462 Wingate, L., Ogee, J., Cuntz, M., Genty, B., Reiter, I., Seibt, U., Yakir, D., Maseyk, K., Pendall,
463 E. G., Barbour, M. M., Mortazavi, B., Burrell, R., Peylin, P., Miller, J., Mencuccini, M., Shim,
464 J. H., Hunt, J. and Grace, J.: The impact of soil microorganisms on the global budget of
465 delta¹⁸O in atmospheric CO₂, *Proc. Natl. Acad. Sci. U. S. A.*, 106(52), 22411–5,
466 doi:10.1073/pnas.0905210106, 2009.
- 467 Wingate, L., Ogee, J., Burrell, R., Bosc, A., Devaux, M., Grace, J., Loustau, D. and Gessler, A.:
468 Photosynthetic carbon isotope discrimination and its relationship to the carbon isotope signals
469 of stem, soil and ecosystem respiration, *New Phytol.*, 188(2), 576–589, doi:10.1111/j.1469-
470 8137.2010.03384.x, 2010.
- 471 Yamaoka, K., Nakagawa, T. and Uno, T.: Application of Akaike's information criterion (AIC)
472 in the evaluation of linear pharmacokinetic equations, *J. Pharmacokinet. Biopharm.*, 6(2), 165–



473 175, doi:10.1007/BF01117450, 1978.

474



1 Table.1 The $\delta^{13}\text{C}$ and $\delta^{18}\text{O}$ values of the calibration standards used measured against VPDB.

2

CO ₂ standard	$\delta^{13}\text{C}$	$\delta^{18}\text{O}$
Heavy standard	$-3.99 \pm 0.03\text{‰}$	$-13.08 \pm 0.06\text{‰}$
Medium standard	$-21.06 \pm 0.03\text{‰}$	$-21.14 \pm 0.024\text{‰}$
Heavy standard	$-38.12 \pm 0.04\text{‰}$	$-29.2 \pm 0.035\text{‰}$

3

4

5

6

7

8

9

10

11

12



Table 2. Correction factor models are fitted for $\Delta\delta^{13}\text{C}$, DF (Degrees of Freedom), AIC_c (Akaike information criterion) and $[\text{CO}_2]$ CO_2 concentration in ppm.

Model Fit	Equation	R^2	AIC_c	DF
Exponential	$\Delta\delta^{13}\text{C} = a * (b - \exp(-c * [\text{CO}_2]))$	0.99	3.79	8
Rational	$\Delta\delta^{13}\text{C} = (a + b * [\text{CO}_2]) / (1 + c * [\text{CO}_2] + d * [\text{CO}_2]^2)$	0.98	7.79	7
Dose - Response	$\Delta\delta^{13}\text{C} = \alpha + \theta * [\text{CO}_2]^\eta / (\kappa^\eta + [\text{CO}_2]^\eta)$	0.98	8.7	7
Sigmoidal	$\Delta\delta^{13}\text{C} = (a * b + c * [\text{CO}_2]^d) / (b + [\text{CO}_2]^d)$	0.98	8.703	7
Logarithmic	$\Delta\delta^{13}\text{C} = a + b * \ln([\text{CO}_2])$	0.92	19.22	9
Lowess	-----	0.85	28.89	8

2
 3
 4
 5
 6
 7



8

9 Table 3. Correction factor models are fitted for $\Delta\delta^{18}\text{O}$, DF (Degrees of Freedom), AIC_c (Akaike information criterion) and [CO₂] CO₂ concentration in ppm.

Model Fit	Equation	R ²	AIC _c	DF
Logarithmic	$\Delta\delta^{18}\text{O} = a + b * \ln([\text{CO}_2])$	0.98	-9.035	9
Rational	$\Delta\delta^{18}\text{O} = (a + b * x) / (1 + c * [\text{CO}_2] + d * [\text{CO}_2]^2)$	0.97	2.75	7
Exponential	$\Delta\delta^{18}\text{O} = a * (b - \exp(-c * [\text{CO}_2]))$	0.95	4.58	8
Lowess	-----	0.90	12.22	8

Table 4. Parameter values for correction factor model fit for $\Delta\delta^{13}\text{C}$ & $\Delta\delta^{18}\text{O}$.

Parameter	Value	Std Error	95% Confidence
a¹³C	23.8	1.2	21.08 - 26.68
b¹³C	0.161	0.02	0.10 - 0.21
c¹³C	0.000403	0.000053	0.000281 - 0.000525
a¹⁸O	-29.4	1.25	-32.26 - -26.60
b¹⁸O	3.26	0.14	2.93 - 3.60



Figure 1

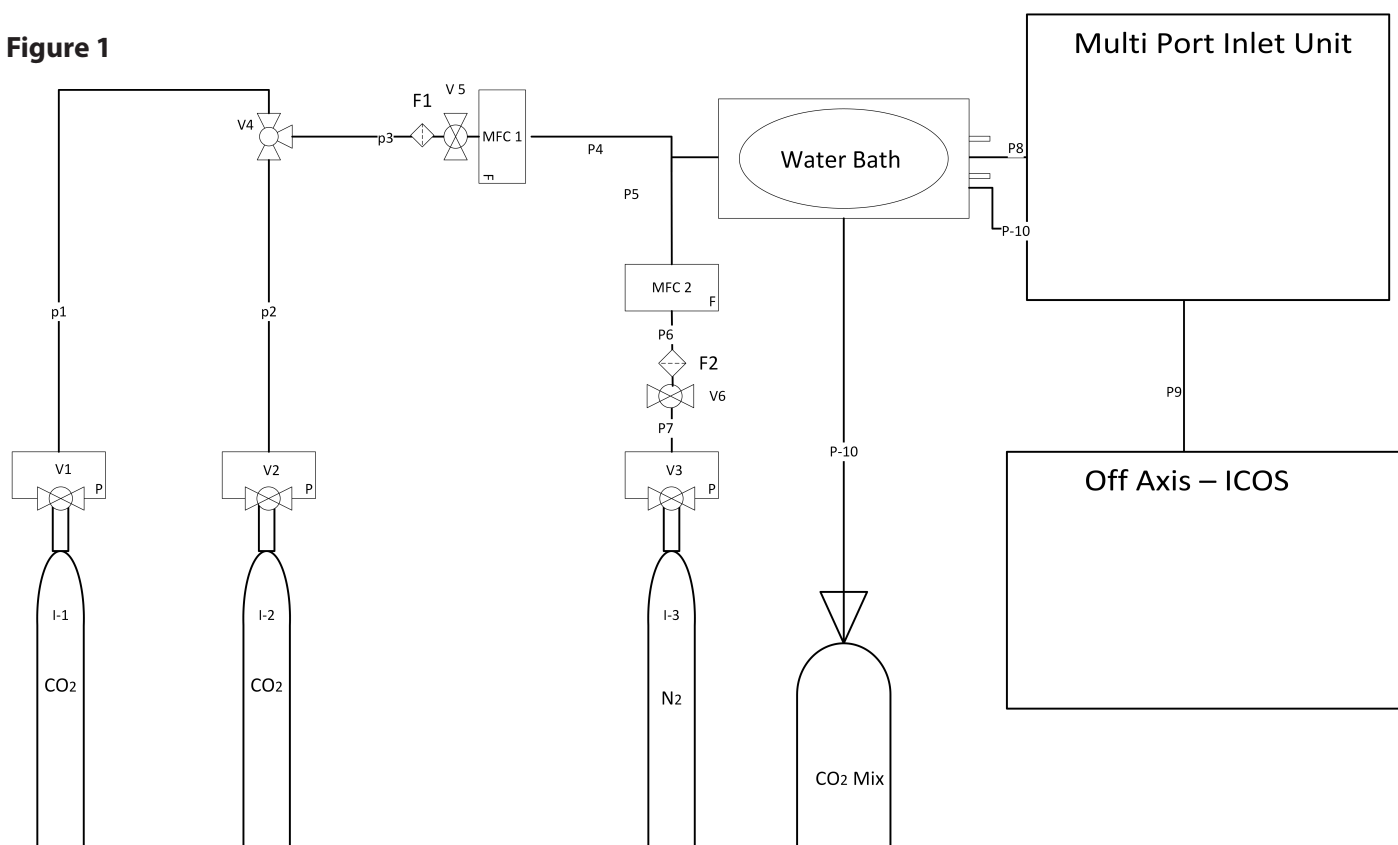


Figure 1: Setup made for calibration of Off Axis ICOS (LGR-CCIA 36-d). I(1,2): CO₂ standards, CO₂ Mix: Gas standards mixed in equal molar proportion, I3: N₂ gas, MFC(1, 2): Mass Flow Controller, F(1, 2): PTFE filter, V(1, 2, 3): Pressure reducing Valves, V4: Three way ball valve, V(5,6): pressure controller valve with safety bypass, P (1-7): Steel pipes, P(8,9,10): ¼" Teflon tubings.



Figure 2

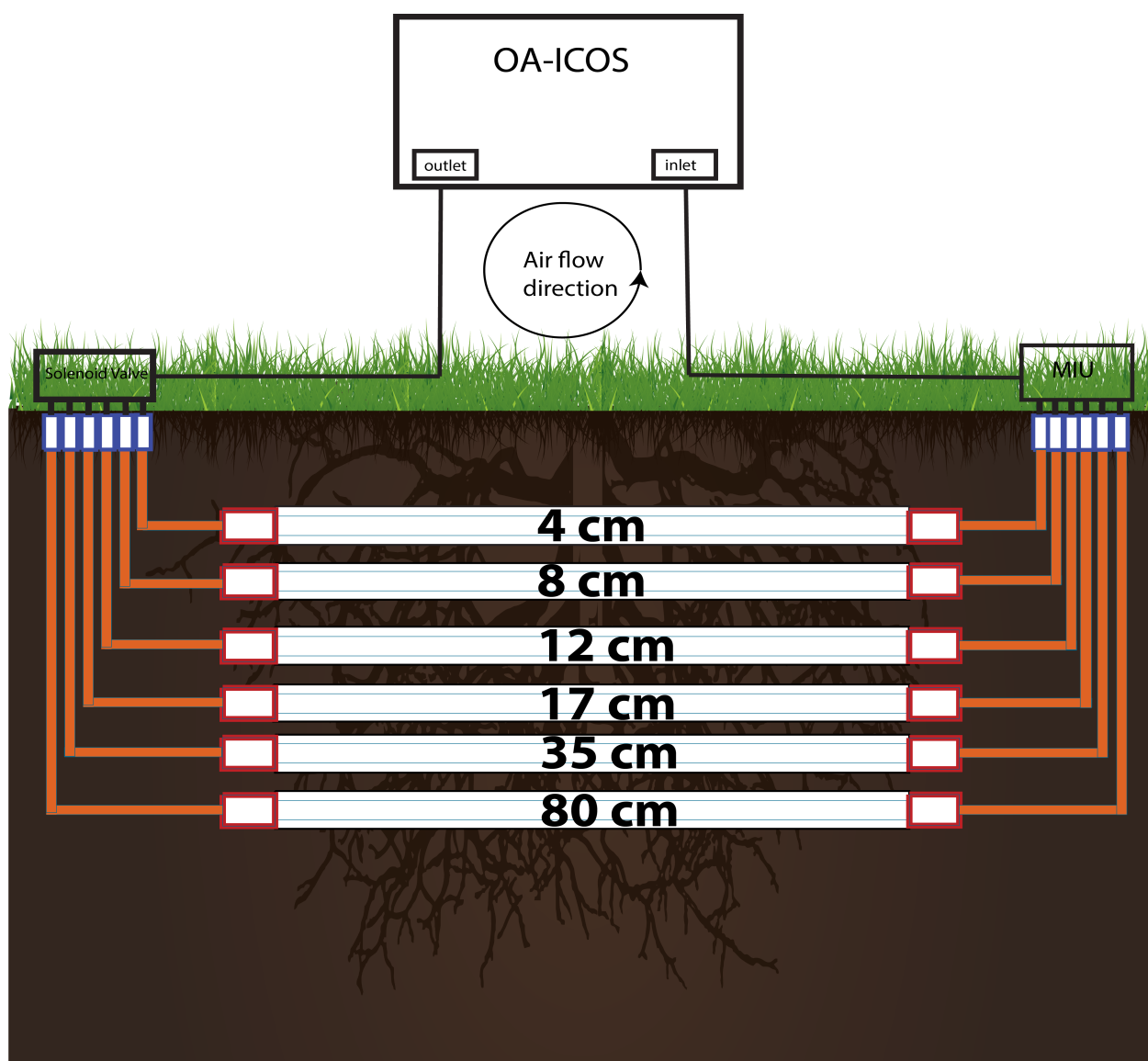


Figure 2: Installation made for soil air CO₂, δ¹³C and δ¹⁸O measurements. MIU represents the multi-port inlet unit. Hydrophobic membrane tubings installed horizontally in soil at different depths.



Figure 3

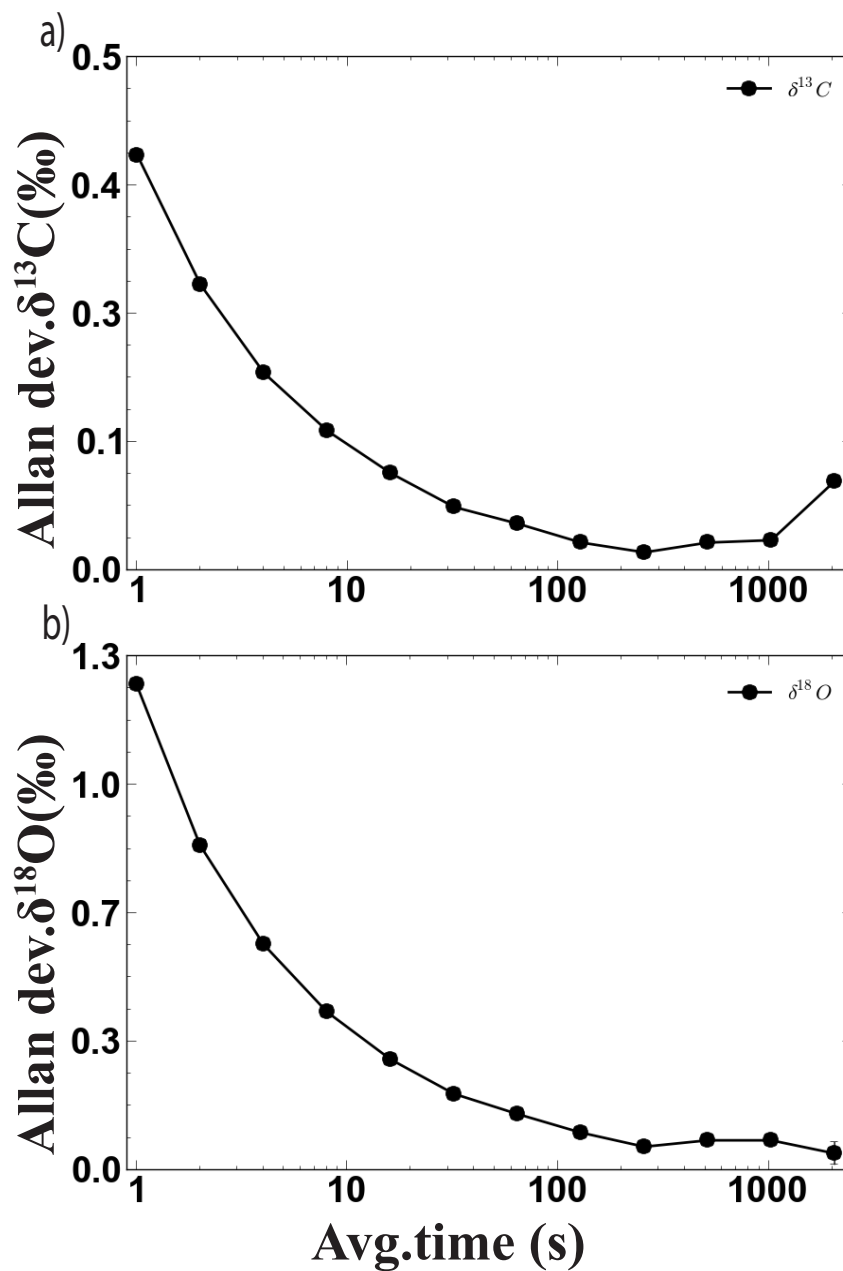


Figure 3: Allan deviation curve for $\delta^{13}C$ (a) and $\delta^{18}O$ (b) measurements by Los Gatos CO₂ Carbon isotope analyzer CCIA-36d.



Figure 4

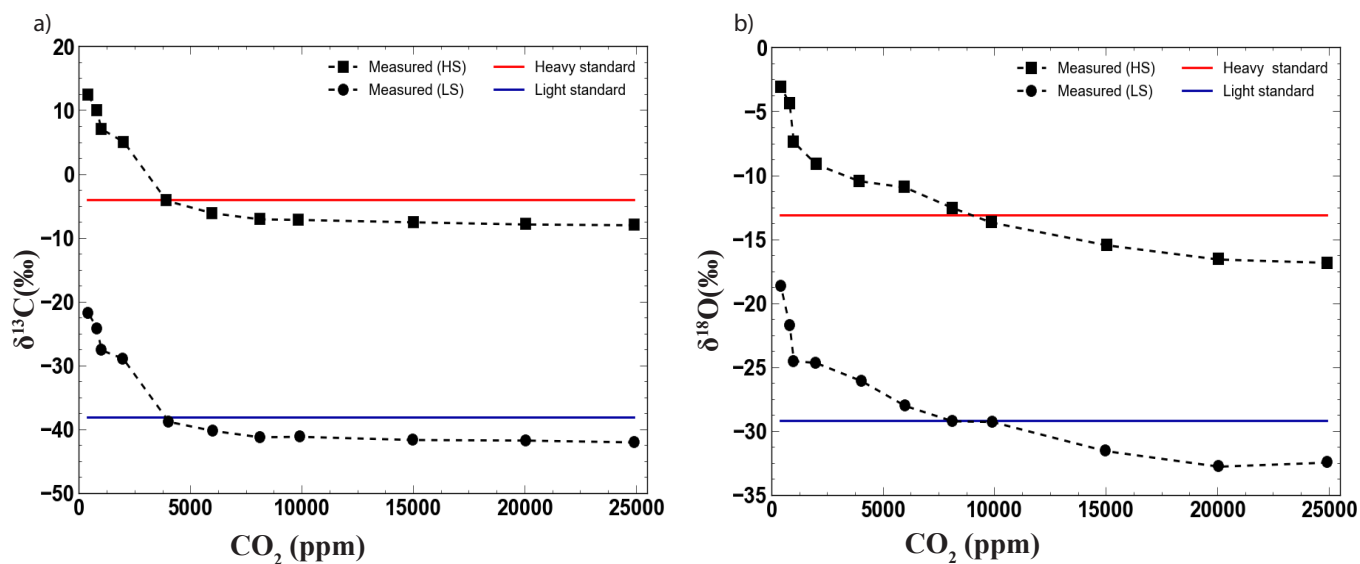


Figure 4: Variability observed in $\delta^{13}\text{C}$ (a) and $\delta^{18}\text{O}$ (b) measurements without calibration. Where measured δ values for Heavy Standard and Light Standard are shown as Measured (HS) and Measured (LS) respectively. Actual δ value for heavy standard and light standard are shown as red and blue line respectively.



Figure 5

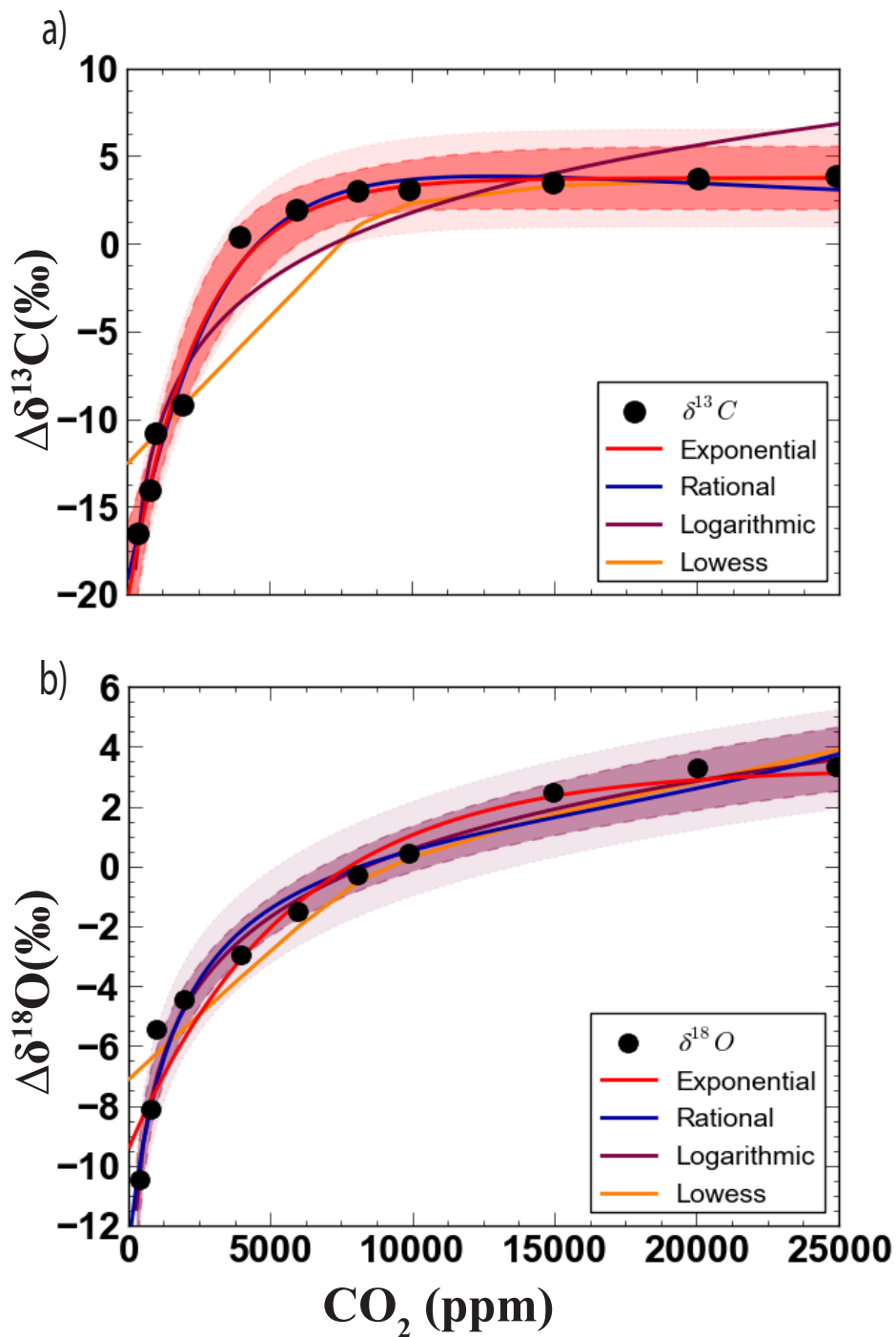


Figure 5: Correction factor model fit for the $\Delta\delta^{13}\text{C}$ (a) & $\Delta\delta^{18}\text{O}$ (b) for Los Gatos CO₂ Carbon isotope analyzer CCI A-36d with 95% confidence interval and a 95% prediction band.



Figure 6

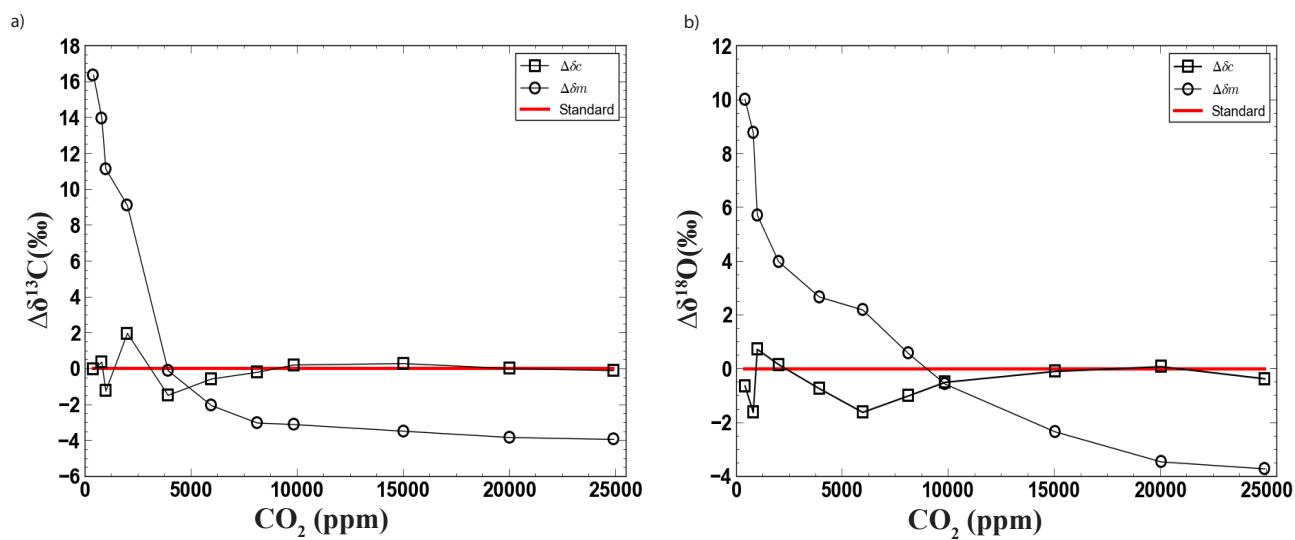


Figure 6: Concentration corrected $\delta^{13}\text{C}$ (a) & $\delta^{18}\text{O}$ (b) measurements by Los Gatos CO₂ Carbon isotope analyzer CCI-36d. Deviation in measured data ($\Delta\delta_m$), deviation in corrected data using model fit ($\Delta\delta_c$), Real value (standard).



Figure 7

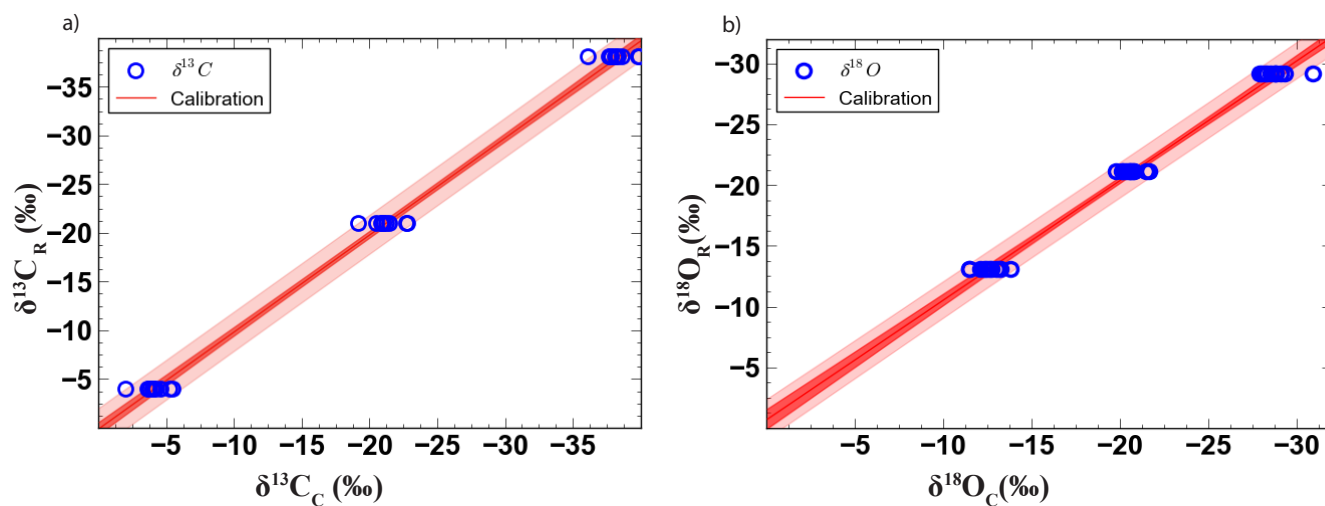


Figure 7: Calibration lines for $\delta^{13}\text{C}$ (a) & $\delta^{18}\text{O}$ (b) by Los Gatos CO_2 Carbon isotope analyzer CCI-36d with 95% confidence interval and a 95% prediction band, where $\delta^{13}\text{C}_R$ and $\delta^{18}\text{O}_R$ denote actual δ values of gas standard and $\delta^{13}\text{C}_C$ and $\delta^{18}\text{O}_C$ stands for δ values corrected for concentration dependency.



Figure 8

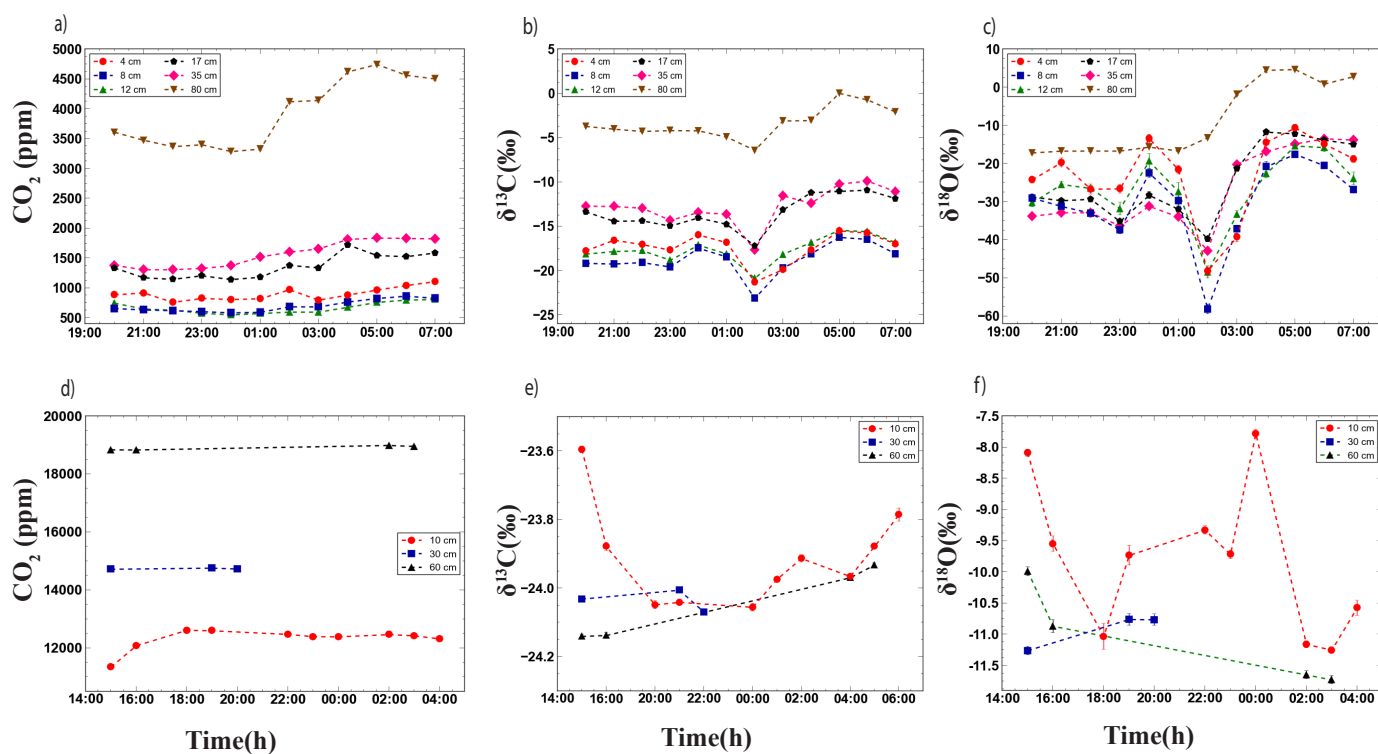


Figure 8: Evolution of soil CO₂ (ppm), δ¹³C and δ¹⁸O in calcareous (a-c) and acidic (d-f) soils.



Figure 9

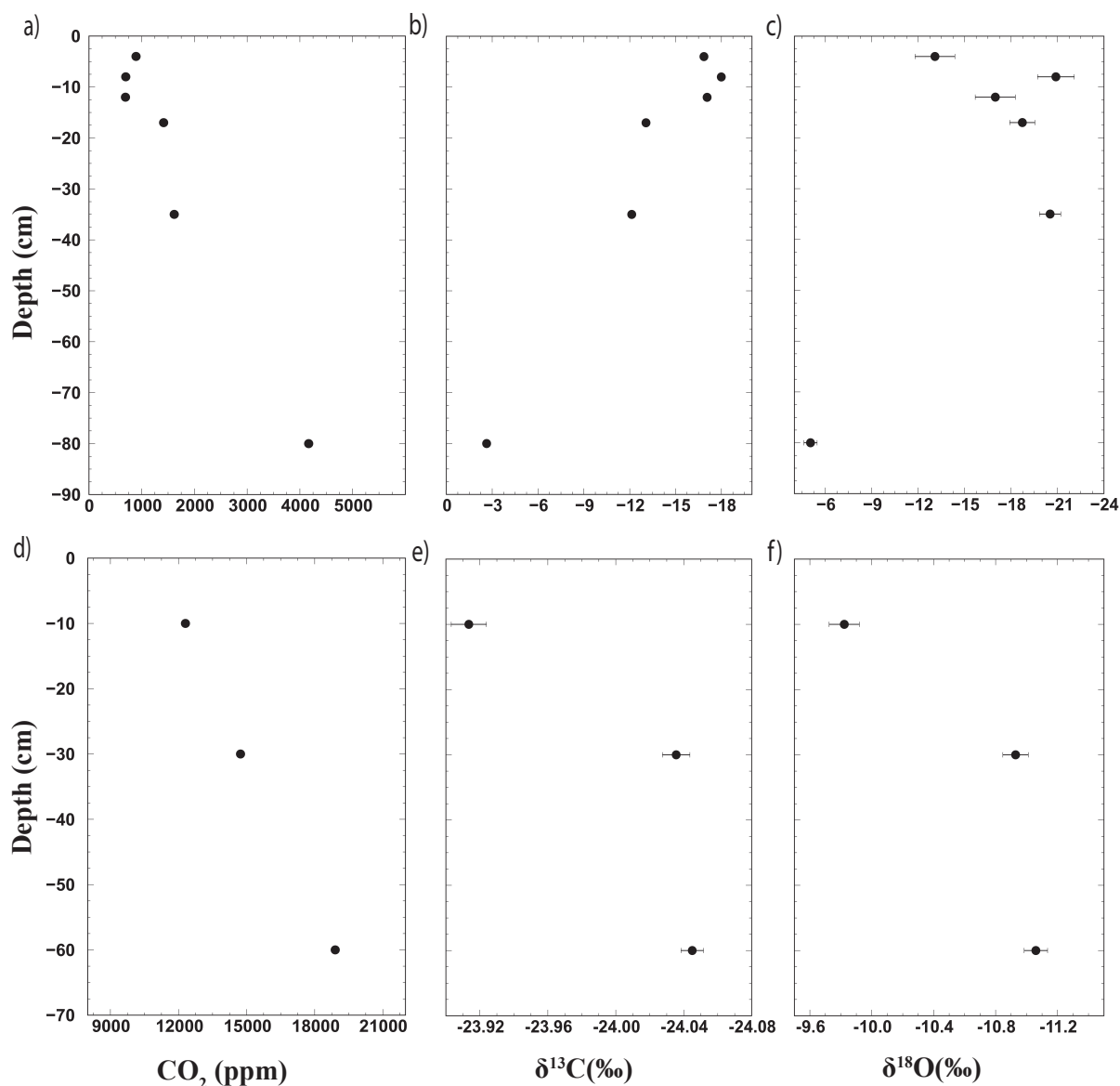


Figure 9: Depth profile of soil air CO₂, δ¹³C and δ¹⁸O. Figures (a-c), shows soil depth profile in calcareous soil and figures (d-f) elucidates soil depth profile in acidic soil.